

PAPER • OPEN ACCESS

Pure single photons from a trapped atom source

To cite this article: D B Higginbottom *et al* 2016 *New J. Phys.* **18** 093038

View the [article online](#) for updates and enhancements.

You may also like

- [Beam steering via peak power decay in nonlinear waveguide arrays](#)

Sotiris Droulias, Yoav Lahini, Yannis Kominis et al.

- [Unconditionally secure digital signatures implemented in an eight-user quantum network](#)

Yoann Pelet, Ittoop Vergheese Puthoor, Natarajan Venkatachalam et al.

- [Coherent spin–rotational dynamics of oxygen superrotors](#)

Alexander A Milner, Aleksey Korobenko and Valery Milner

New Journal of Physics

The open access journal at the forefront of physics

Deutsche Physikalische Gesellschaft 

IOP Institute of Physics

Published in partnership with: Deutsche Physikalische Gesellschaft and the Institute of Physics



OPEN ACCESS

PAPER

Pure single photons from a trapped atom source

D B Higginbottom^{1,2}, L Slodička³, G Araneda², L Lachman³, R Filip³, M Hennrich² and R Blatt^{2,4}

¹ Australian National University, Canberra ACT 0200, Australia

² Institut für Experimentalphysik, Universität Innsbruck, Technikerstr. 25, A-6020 Innsbruck, Austria

³ Department of Optics Palacký University, 17. Listopadu 12, 77146 Olomouc, Czech Republic

⁴ Institut für Quantenoptik und Quanteninformation, Österreichische Akademie der Wissenschaften, Technikerstraße 21a, A-6020 Innsbruck, Austria

E-mail: daniel.higginbottom@anu.edu.au

Keywords: single-photon source, quantum non-Gaussian, trapped ion

Supplementary material for this article is available [online](#)

RECEIVED
11 May 2016

REVISED
23 August 2016

ACCEPTED FOR PUBLICATION
26 August 2016

PUBLISHED
20 September 2016

Original content from this work may be used under the terms of the Creative Commons Attribution 3.0 licence.

Any further distribution of this work must maintain attribution to the author(s) and the title of the work, journal citation and DOI.



Abstract

Single atoms or atom-like emitters are the purest source of single photons, they are intrinsically incapable of multi-photon emission. To demonstrate this degree of photon number-state purity we have realized a single-photon source using a single ion trapped at the common focus of high numerical aperture lenses. Our trapped-ion source produces single-photon pulses with $g^2(0) = (1.9 \pm 0.2) \times 10^{-3}$ without any background subtraction. After subtracting detector dark counts the residual $g^2(0)$ is less than 3×10^{-4} (95% confidence interval). The multi-photon component of the source light field is low enough that we measure violation of a quantum non-Gaussian state witness, by this characterization the source output is indistinguishable from ideal attenuated single photons. In combination with efforts to enhance collection efficiency from single emitters, our results suggest that single trapped ions are not only ideal stationary qubits for quantum information processing, but promising sources of light for scalable optical quantum networks.

Introduction

Light fields of a definite, single excitation are an elementary tool for quantum information and a key feature in schemes for encoding, manipulating and communicating quantum information. A number of protocols for unconditionally secure communication harness the indivisibility of single photon states to distribute an unread cryptographic key (QKD) [1, 2]. Long-distance QKD requires remote entanglement distributed over optical repeater networks, and these in turn require further quantum optical resources. To scale effectively with distance single-photon repeater nodes must be capable of producing single photons with a critically low multi-photon component [3, 4]. The search for low noise single-photon sources is further motivated by their proposed application in systems for performing quantum simulations [5] and computing quantum algorithms without an efficient classical equivalent [6, 7].

An ideal single photon source emits a single photon (and never more than one photon) on demand with 100% probability, at an arbitrarily high rate, and indistinguishable both from previous emissions and from parallel sources [8]. A common source of photons for quantum information experiments [9] is spontaneous parametric down conversion (SPDC) which probabilistically produces correlated pairs of photons across two modes, one of which can be used to herald a single photon in the other. Unless efficient photon number resolving detectors are available to discriminate single-pair from multi-pair events at the herald, SPDC sources produce fields with an intrinsic multi-photon component that scales with the pair generation rate [10] which is detrimental for applications in quantum networks [11]. Correlated photon pairs can also be produced using four-wave mixing (FWM) in waveguides or fibers, although Raman scattering produces problematic background noise.

Single emitters, with no inherent capacity to produce multiple photons simultaneously, are more natural candidates for producing pure single-photon fields. Of these, atoms are appealing because the availability of

identical systems guarantees the possibility of multiplexed indistinguishable photons [12–14]. Atom–photon networks have already exploited the indistinguishability of atomic photon sources with great success [15] for the generation of entanglement [16, 17] and quantum teleportation [18]. The outstanding challenge for single-atom sources is to efficiently capture photons in a convenient spatial mode, although rapid progress is being made with high-finesse cavities and large numerical aperture optics [19–23].

Neutral atoms with Λ -type level schemes have been optically trapped inside high-finesse cavities for the production of photons by fast excitation [24] and vacuum stimulated Raman adiabatic passage (STIRAP) [25–29]. The single photon production probability in such a system is limited by the cavity mode density and optical cavity losses. Shallow optical traps further compromise neutral atom systems; the trap must be reloaded during operation and the possibility of capturing more than one atom contributes a multi-photon probability. In contrast, ion sources in radio frequency (RF) traps can be held for longer and confined more tightly. A charged particle source poses some challenges for strong cavity coupling, but both STIRAP and far off resonant Raman schemes have been implemented in ion-cavity systems [30, 31].

Artificial atoms such as semiconductor quantum dots (QDs) [32, 33] can be integrated with optical microcavities [34–37] to improve collection efficiency. While QDs are in principle single emitters, multi-photon noise in these systems is typically present due to interactions with the bulk material [38] and needs to be suppressed [39]. Scalable quantum dot networks require either the capacity to tune multiple dots for mutually indistinguishable photons [40], or a single dot producing long streams of indistinguishable photons [41] that can be demultiplexed across many spatial modes. Nitrogen vacancy (NV) centers in diamond nanocrystals are an alternative with similar noise challenges.

To compare the performance of single-photon sources it is necessary to have a measure of quantum behavior that captures the useful properties of the single photon field. A ubiquitous number-state measurement of the single photon field is the degree of anticorrelation $\alpha = P_c/P_s^2$ measured in a Hanbury Brown–Twiss (HBT) experiment, where P_s and P_c are the probability of single detection events and coincidence events respectively. For small mean photon flux the light field intensity autocorrelation $g^{(2)}(\tau)$ reduces to α when $\tau = 0$ [42, 43]. $\alpha < 1$ is a signature of non-classical light states, however this is just the first in a hierarchy of more stringent quantum signatures that can be used to test the performance of a single photon source [44] and neglects the vacuum component of the optical state, which crucially characterizes the efficiency, η , of on-demand photon sources [3].

The negativity of the Wigner function is a stricter criterion for non-classicality and a necessary quantum computational resource [45]. Wigner function negativity is a distinguishing property of all pure quantum non-Gaussian (QNG) states [46], including ideal single-photon states. However, while a strongly attenuated field is necessarily non-negative in the Wigner representation, QNG remains an unambiguous and efficient test of higher-order quantum behavior even for mixed or attenuated states [47]. Indeed, QNG is a sufficient condition for security in realistic models of discrete-variable QKD networks [48]. The same HBT configuration as a typical $g^{(2)}(\tau)$ measurement [49] is sufficient for estimation of a QNG witness that distinguishes light fields from any convex mixture of coherent and squeezed states [50]. Beating such a QNG threshold is therefore a necessary benchmark for applications in quantum information processing and a sufficient benchmark for realistic QKD networks. This has stimulated several recent characterizations of single photon sources using the QNG measure for efficient but noisy sources [47, 51].

In this work we develop and characterize an experimental scheme for the generation of low-noise single photons using a single trapped ion at the focus of high numerical aperture lenses under pulsed excitation. We apply both the conventional $g^{(2)}(0)$ and a new QNG metric to demonstrate that our source produces a single-photon light field with critically low noise sufficient for scalable networks. The source performs with near optimal QNG witness depth and is limited solely by the dark count rate of the detection technology available at this wavelength.

Methods

A $^{138}\text{Ba}^+$ ion is trapped and cooled in a linear Paul trap at the common focus of two high aperture lens objectives (HALOs) as per figure 1. The ion is Doppler cooled to within the Lamb–Dicke regime using a 493 nm cooling laser and a repump beam at 650 nm to close the $6\text{S}_{1/2}$ – $6\text{P}_{1/2}$ – $5\text{D}_{3/2}$ cycle, figure 1 (inset). Three pairs of Helmholtz coils create a magnetic field that defines the atomic quantization axis of the radiating dipole at 90° to the common axis of the cooling and repump beams and lifts the degeneracy of the three atomic levels in the simple Λ scheme in figure 1 such that the complete system dynamics is described by a set of eight-level Bloch equations. Each HALO has a numerical aperture of 0.4 and together they collect a combined 12% of the ion’s dipole fluorescence on the 493 nm Doppler cooling transition.

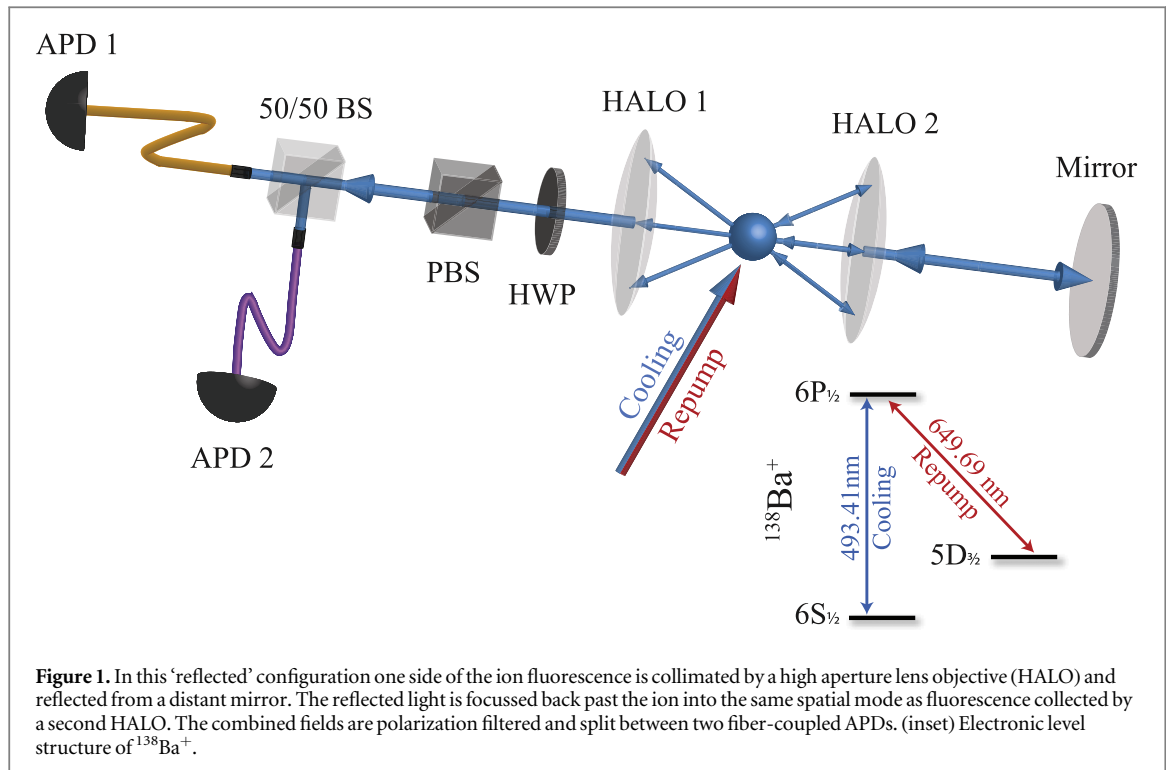


Figure 1. In this ‘reflected’ configuration one side of the ion fluorescence is collimated by a high aperture lens objective (HALO) and reflected from a distant mirror. The reflected light is focussed back past the ion into the same spatial mode as fluorescence collected by a second HALO. The combined fields are polarization filtered and split between two fiber-coupled APDs. (inset) Electronic level structure of $^{138}\text{Ba}^+$.

The detectors are configured for a HBT measurement with one reflected field; two low-noise fiber-coupled APDs with quantum efficiencies of 70% and 73% on either arm of a 50/50 beamsplitter sample a single spatial and polarization mode of the ion fluorescence collected by one of the HALOs. Fluorescence collected by the second HALO is back-reflected over the ion by a distant mirror such that it too is collected by the same APDs. The ion fluorescence in this configuration self-interferes with 90% visibility when sideband cooled [52] and 70% visibility when Doppler cooled as it is here [53]. It is possible to lock the ion-mirror path length such that constructive interference enhances the detection efficiency [52]. However, the results presented here are recorded with the mirror position freely scanning such that self-interference effects average out. This will allow us to compare a QNG witness across multiple modes. Detection events at the APDs are time tagged using a photon counting module with a time resolution of 4 ps.

Photons are produced by pulsing the cooling and repump beams according to the scheme shown in figure 2(a), similar to the operation of [54, 55], at an attempt rate of $2 \times 10^5 \text{s}^{-1}$. The experimental sequence begins with $2 \mu\text{s}$ of Doppler cooling by both the cooling and repump beams. The ion is prepared in a statistical mixture of the $D_{3/2}$ shelving states by $1 \mu\text{s}$ of driving with only the cooling beam. Both beams are off for 500 ns before the repump is switched back on to trigger the spontaneous emission of an unpolarized 493 nm photon. Polarization filtering reduces the detection probability by 2/3 in the chosen polarization mode. In figure 2(b) we show arrival time histograms of Raman photons as the repump power is steadily increased to the transition saturation point. The initial state mixture produces frequency mixed photons with a corresponding increase in distinguishability proportional to the magnetic field. For applications requiring a high degree of indistinguishability it is necessary to prepare a well-defined state. An identical Raman scheme using the $6\text{S}_{1/2}$ – $6\text{P}_{3/2}$ – $5\text{D}_{5/2}$ cycle (for example) would produce polarized photons if the ion was first prepared in a single extremal $D_{5/2}$ Zeeman state [54].

The magnetic field (\vec{B}) is calibrated by spectroscopy of the quadrupole transition $6\text{S}_{1/2} \rightarrow 5\text{D}_{5/2}$ using a fiber-coupled $1.7 \mu\text{m}$ laser locked to a narrow linewidth cavity. The cooling and repump beam powers (Ω_g, Ω_r), the detuning (Δ_g) and common polarization (\vec{P}) are inferred from a spectroscopic dark state measurement prior to operation. Eight-level Bloch simulations predict the stationary fluorescence rate as a function of Δ_r and the above parameters are fitted to the corresponding measurement, see figure 2(c). The same Bloch equations can then be used to calculate the dynamic single-photon scattering rate as a function of time after the repump is switched on under the driving scheme in figure 2(a), with repump beam parameters ($\Omega_r, \Delta_r, \vec{P}$) inferred from the continuous-driving dark state scan. This dynamic simulation takes into account the intensity profile of the repump beam (rise time 90 ns) as measured after the switching/shaping AOM, and assumes that the preparation

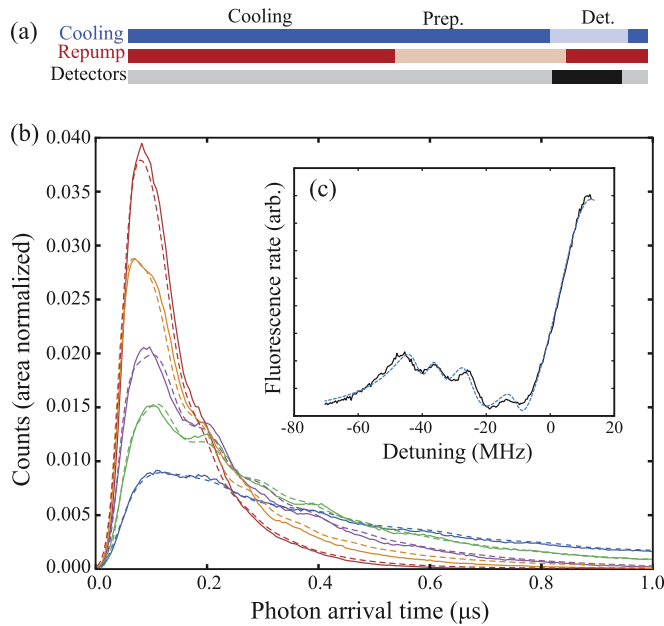


Figure 2. (a) The Raman driving scheme that is used to cool, prepare and trigger the trapped ion photon source. Single photon pulses are produced by alternating the cooling (blue) and repump (red) beams. Both beams are on for most of the cycle to Doppler cool the ion. During the preparation stage the repump beam is switched and the ion's electron is shelved in a $D_{3/2}$ dark state. A single blue photon is emitted using only the repump beam and detected by fiber coupled APDs. (b) Area normalized histograms of single-photon arrival times using the above scheme. These intensity distributions show the mean arrival time decreasing as the repump beam power Ω_r is steadily increased to the transition saturation point. The eight-level Bloch model of our system predicts corresponding single photon shapes shown by dashed lines. For each trace the model parameters are calibrated using a dark resonance scan under the same driving conditions. A typical example of the dark resonance parameter fit is shown in inset (c) with the measured fluorescence rate (solid black line) and fit from the model (dashed blue line) with parameters corresponding to the slowest (blue) single photon shape.

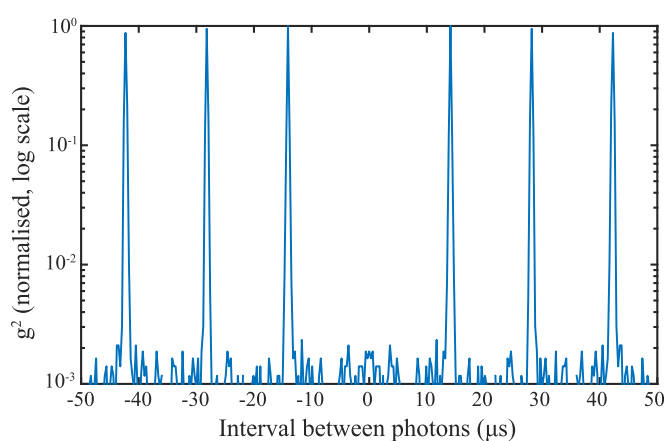


Figure 3. Intensity auto-correlation ($g^2(\tau)$) of the pulsed resonance fluorescence when the trapped-ion single photon source is operated at a rate of $7 \times 10^4 \text{ s}^{-1}$. The data is presented without background subtraction and shows $g^2(0) = (1.9 \pm 0.2) \times 10^{-3}$. The pulsed source is triggered according to the scheme in (figure 2(b)) but at one third of the trigger rate so that a statistically significant amount of background can be measured during an extended detection window. Fluorescence in the cooling periods between the photon generation windows has been removed.

process leaves the ion in a mixed state with probabilities equally distributed between the four $5D_{3/2}$ levels and with no coherences between that manifold.

The eight-level optical Bloch model predicts dynamic scattering probabilities in close agreement with the measured single photon wavepacket (figure 2(a)). The arrival time distribution features a distinctive oscillation at a frequency independent of the repump beam power. These quantum beats are caused by interference between $6P_{1/2}$ – $5D_{3/2}$ absorption amplitudes that enhances and suppresses the emission of Raman-scattered $6S_{1/2}$ – $6P_{1/2}$ photons in the detection mode with frequency determined by the D state energy splitting [56].

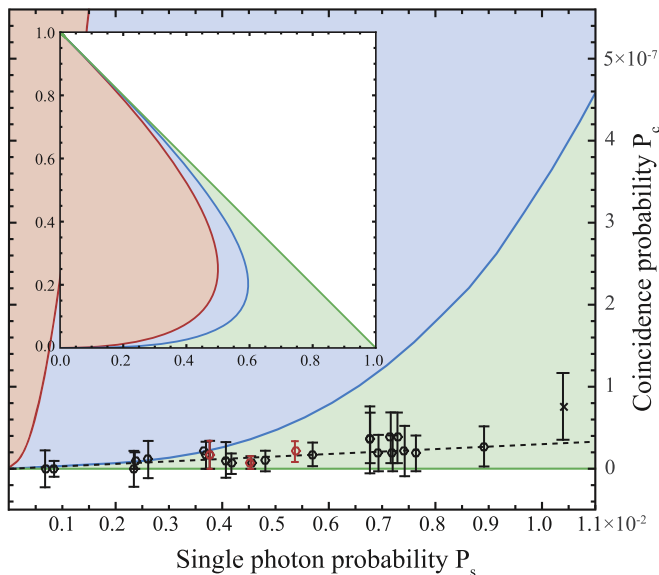


Figure 4. Coincidence probability P_c versus single photon detection probability P_s in the operational region of our source and over the complete phase space (inset). Classical light coincidence rates cannot be reduced below the NC threshold (red) and Gaussian light fields are similarly restricted to coincidence rates above the QNG threshold (blue). Light fields with coincidence rates below this threshold (green region) are unambiguously QNG. Circles correspond to measurements of our pulsed single-photon source in the reflected (red) and symmetric (black) configuration with a 200 ns detection window and under a range of driving conditions. The black cross is a measurement under optimal conditions with a 500 ns detection window. Error bars represent 95% confidence intervals. The dashed line predicts the performance of an ideal single-photon source measured with our detectors and a 200 ns detection window.

Results

The second order intensity correlation function $g^2(0) = 0.0019(2)$ of the field emitted by our photon source violates the coherent state condition $\alpha \leq 1$ under continuous and pulsed driving (figure 3). The measured α corresponds precisely to the stated and measured dark count rate of our two detectors, 10 ± 2 counts s^{-1} per detector. By subtracting this measured dark count rate from the measured coincidences we can say with 95% confidence that the intrinsic α of our source is below 3×10^{-4} .

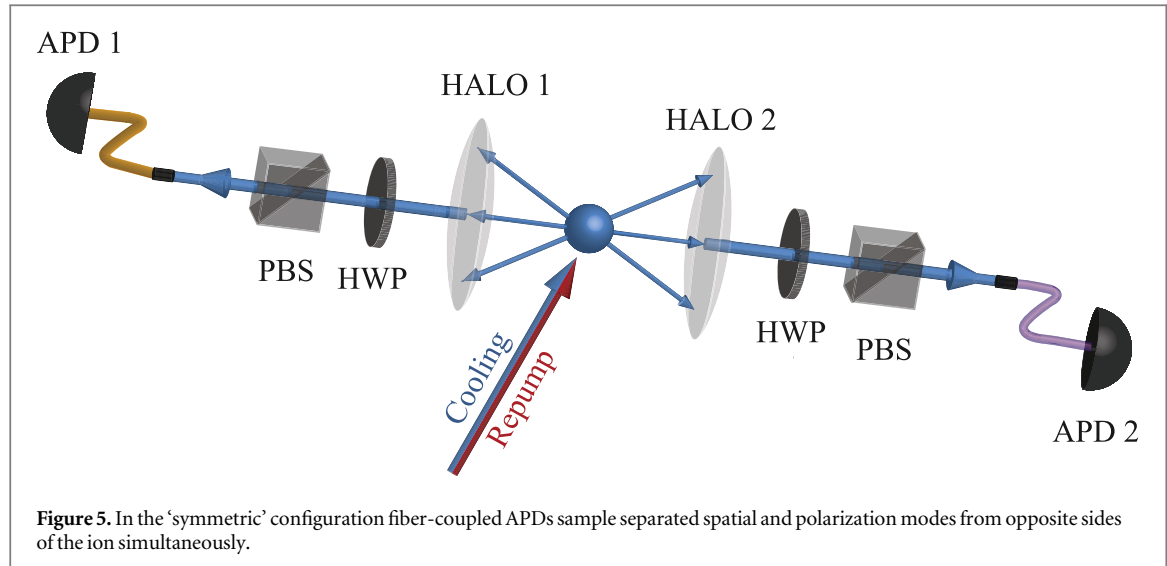
In numerical models of discrete-variable quantum repeater networks the possible network size is critically bounded by the multi-photon component. In [3] the authors consider the entanglement-based QKD network of [57] and show that even a small multiple-pair probability can be extremely detrimental. An otherwise ideal network of efficient photon sources with $\eta = 0.9$ and $\alpha = 0.01$ becomes useless for QKD at any rate after only seven concatenated network links. In contrast, an efficient trapped atom source with the same α and dark noise-rate as our source may support high QKD rates over up to thirty network links.

In this work the efficiency of the source is limited by the collection proportion of the two HALOs, polarization filtering, detection efficiency, and fiber coupling efficiency so that the end-to-end efficiency is $\eta = 0.0054$. However the initial light field is so close to a perfect single-photon Fock state that higher-order quantum behavior is evident even after this high degree of attenuation. We demonstrate this higher order quantum behavior by showing that the measured photon statistics violate a QNG optical state witness [50]. Following [58], both the traditional non-classicality (NC) criteria $\alpha < 1$ and this QNG witness can be formulated in terms of probabilities P_s and P_c measured in an optical HBT configuration. Classical states (states that can be written as a mixture of coherent states) are bounded by the inequality $P_s \leq 2(\sqrt{P_c} - P_c)$ illustrated by the red curve in figure 4 (inset). A stricter threshold can be calculated for Gaussian states [58], blue curve in figure 4 (inset). The QNG threshold can be written for these observables in an implicit form parametrized by the degree of squeezing (V) of the threshold states (derivation presented in supplementary material)

$$P_s = \frac{1}{2} + \frac{(1 - V(2 + V))e^{\frac{V-1}{2V}}}{\sqrt{V}(1 + V)^2}, \quad (1)$$

$$P_c = \frac{1}{2} - \frac{(1 + V^2)e^{\frac{V-1}{2V}}}{\sqrt{V}(1 + V)^2}. \quad (2)$$

In the operational region of our source this threshold can be reduced to $P_c \approx P_s^3/3$, see figure 4. Any state with single-mode coincidence probability P_c below this threshold is unambiguously QNG. Due to strong



attenuation our source sits in a corner of the P_s, P_c phase space. Nevertheless, because our source is low-noise it beats the QNG threshold by 6 standard deviations in the optimal configuration as depicted in figure 4 (red circles). The number of detections and coincidences are determined in a detection window 200 ns long from the beginning of the photon trigger. These measurements further confirm an excellent quality of the generated single photons, with performance limited solely by the overall single-photon collection efficiency and detector dark counts.

The typical approach to enhancing collection efficiency from low-efficiency single photon emitters employs combinations of high numerical aperture optical elements [13, 23, 59–61]. This corresponds to simultaneous emission of a light field into several spatial modes. Such a multi-mode source is useful so long as the purity of emitted single-photons is not compromised. Simultaneous enhancement of spurious background light collection, spatial restrictions on excitation beams, excitation beam scattering into the photon collection modes and other processes can in general make enhancing collection efficiency a source of additional photon-number noise. To estimate this effect, we measure the same QNG witness for a light state emitted coherently by a single-photon source into two spatial modes. We apply this measure to our single trapped ion source as presented in figure 5. The fluorescence is detected in two spatial directions by APDs positioned behind each HALO lens. In the reflected configuration, the collected photons were forced to enter the same spatial mode prior to the detection, in the symmetric setup they are emitted into two, in principle independent, directions. As demonstrated in [52, 53], ion fluorescence emitted in two opposite directions remains phase coherent to a very high degree and can be efficiently transferred into a single spatial mode, for example by recombination on a beamsplitter. The single ion in the symmetric configuration thus comprises both the emitter and perfect unitary beamsplitter of the typical Hanbury Brown–Twiss measurement configuration. The QNG measurements presented for our source emitting into a single spatial mode can be compared to two-mode coincidence measurement evaluated to yield the same measure.

Measurements made in the symmetric configuration with a detection window of 200 ns, figure 4 (black circles) suggest that fluorescence collected across two modes remains very close to an ideal single-photon Fock state, more than 20 s.d. from the QNG threshold. Optical losses are lower in this configuration and the fiber coupling is more efficient, improving the end-to end efficiency $\eta = 0.0089$. Increasing the detection window to 500 ns, figure 4 (black x), further improves the efficiency to $\eta = 0.0104$ (albeit with coincidence rate increasing with window size). These measurements indicate that the techniques currently being pursued to increase collection efficiency from single emitters in free space would not have any detrimental effect on the number state of the collected photons.

Conclusion

In both symmetric and reflected configurations, and for a wide range of driving conditions, this trapped-ion photon source produces a pulsed light field with coincidence rates indistinguishable from an ideal single-photon Fock state measured with our detectors, see figure 4 (dashed line). Single-atom photon sources are therefore sufficiently pure for applications in even large quantum networks, without the need for highly multimode

quantum memories, photon number discriminating detectors or entanglement distillation [3, 11]. Even the low efficiency source presented here is demonstrably QNG, the first such demonstration for a single atom source, and therefore sufficient for secure QKD [48]. Although trapped atoms are a spectrally bright source of indistinguishable photons and have already been used in rudimentary quantum networks [16–18] it remains to be seen whether they can be coupled efficiently to network links. However, the efficiency of single-atom optical coupling is progressing rapidly [19, 23, 62–64] and our work suggests that efficient collection is possible across multiple spatial modes without any detriment to the single-photon number state. In addition to being excellent stationary qubits, trapped single atoms are promising photon sources for practical quantum photonic networks.

Acknowledgments

The work reported here has been supported by the Austrian Science Fund FWF (SINFONIA, SFB FoQuS), by the European Union (CRYPTERION #227959), and by the Institut für Quanteninformation GmbH. LS and RF acknowledge financial support from grant No. GB14-36681G of the Czech Science Foundation.

References

- [1] Bennett C H and Brassard G 1984 Quantum cryptography: public key distribution and coin tossing *Theor. Comput. Sci.* **175** 8
- [2] Ekert A K 1991 Quantum cryptography based on Bell's theorem *Phys. Rev. Lett.* **67** 661–3
- [3] Guha S, Krovi H, Fuchs C A, Dutton Z, Slater J A, Simon C and Tittel W 2015 Rate-loss analysis of an efficient quantum repeater architecture *Phys. Rev. A* **92** 022357
- [4] Khalique A and Sanders B C 2015 Practical long-distance quantum key distribution through concatenated entanglement swapping with parametric down-conversion sources *J. Opt. Soc. Am. B* **32** 2382–90
- [5] Georgescu I M, Ashhab S and Nori F 2014 Quantum simulation *Rev. Mod. Phys.* **86** 153–85
- [6] Knill E, Laflamme R and Milburn G J 2001 A scheme for efficient quantum computation with linear optics *Nature* **409** 46–52
- [7] Kok P, Nemoto K, Ralph T C, Dowling J P and Milburn G J 2007 Linear optical quantum computing with photonic qubits *Rev. Mod. Phys.* **79** 135–74
- [8] Eisaman M D, Fan J, Migdall A and Polyakov S V 2011 Invited review article: single-photon sources and detectors *Rev. Sci. Instrum.* **82** 071101
- [9] Soujaeff A, Nishioka T, Hasegawa T, Takeuchi S, Tsurumaru T, Sasaki K and Matsui M 2007 Quantum key distribution at 1550 nm using a pulse heralded single photon source *Opt. Express* **15** 726
- [10] Wakts E, Diamanti E and Yamamoto Y 2006 Generation of photon number states *New J. Phys.* **8** 4
- [11] Krovi H, Guha S, Dutton Z, Slater J A, Simon C and Tittel W 2016 Practical quantum repeaters with parametric down-conversion sources *Appl. Phys. B* **122** 52
- [12] Maunz P, Moehring D L, Olmschenk S, Younge K C, Matsukevich D N and Monroe C 2007 Quantum interference of photon pairs from two remote trapped atomic ions *Nat. Phys.* **3** 538–41
- [13] Gerber S, Rotter D, Hennrich M, Blatt R, Rohde F, Schuck C, Almendros M, Gehr R, Dubin F and Eschner J 2009 Quantum interference from remotely trapped ions *New J. Phys.* **11** 013032
- [14] Legero T, Wilk T, Hennrich M, Rempe G and Kuhn A 2004 Quantum beat of two single photons *Phys. Rev. Lett.* **93** 070503
- [15] Moehring D L, Madsen M J, Younge K C, Kohn R N Jr, Maunz P, Duan L-M, Monroe C and Blinov B B 2007 Quantum networking with photons and trapped atoms (Invited) *J. Opt. Soc. Am. B* **24** 300
- [16] Moehring D L, Maunz P, Olmschenk S, Younge K C, Matsukevich D N, Duan L-M and Monroe C 2007 Entanglement of single-atom quantum bits at a distance *Nature* **449** 68–71
- [17] Slodička L, Hétet G, Röck N, Schindler P, Hennrich M and Blatt R 2013 Atom–atom entanglement by single-photon detection *Phys. Rev. Lett.* **110** 083603
- [18] Olmschenk S, Matsukevich D N, Maunz P, Hayes D, Duan L-M and Monroe C 2009 Quantum teleportation between distant matter qubits *Science* **323** 486–9
- [19] Maiwald R, Golla A, Fischer M, Bader M, Heugel S, Chalopin B, Sondermann M and Leuchs G 2012 Collecting more than half the fluorescence photons from a single ion *Phys. Rev. A* **86** 043431
- [20] Leuchs G and Sondermann M 2012 Lightmatter interaction in free space *J. Mod. Opt.* **20** 1–7
- [21] Slodička L, Hétet G, Hennrich M and Blatt R 2015 Free space interference experiments with single photons and single ions *Engineering the Atom-Photon Interaction: Controlling Fundamental Processes with Photons, Atoms and Solids: Quantum Physics* (Cham: Springer) pp 99–124
- [22] Monroe C and Kim J 2013 Scaling the ion trap quantum processor *Science* **339** 1164–9
- [23] Noek R, Vrijen G, Gaultney D, Mount E, Kim T, Maunz P and Kim J 2013 High speed, high fidelity detection of an atomic hyperfine qubit *Opt. Lett.* **38** 4735
- [24] Bochmann J, Mücke M, Langfahl-Klabes G, Erbel C, Weber B, Specht H P, Moehring D L and Rempe G 2008 Fast excitation and photon emission of a single-atom-cavity system *Phys. Rev. Lett.* **101** 223601
- [25] Kuhn A, Hennrich M and Rempe G 2002 Deterministic single-photon source for distributed quantum networking *Phys. Rev. Lett.* **89** 067901
- [26] McKeever J, Boca A, Boozer A D, Buck J R and Kimble H J 2003 Experimental realization of a one-atom laser in the regime of strong coupling *Nature* **425** 268–71
- [27] McKeever J, Boca A, Boozer A D, Miller R, Buck J R, Kuzmich A and Kimble H J 2004 Deterministic generation of single photons from one atom trapped in a cavity *Science* **303** 1992–4
- [28] Nisbet-Jones P B R, Dilley J, Ljunggren D and Kuhn A 2011 Highly efficient source for indistinguishable single photons of controlled shape *New J. Phys.* **13** 103036
- [29] Mücke M, Bochmann J, Hahn C, Neuzner A, Nölleke C, Reiserer A, Rempe G and Ritter S 2013 Generation of single photons from an atom-cavity system *Phys. Rev. A* **87** 063805

- [30] Keller M, Lange B, Hayasaka K, Lange W and Walther H 2004 Continuous generation of single photons with controlled waveform in an ion-trap cavity system *Nature* **431** 1075–8
- [31] Barros H G, Stute A, Northup T E, Russo C, Schmidt P O and Blatt R 2009 Deterministic single-photon source from a single ion *New J. Phys.* **11** 103004
- [32] Shields A J 2007 Semiconductor quantum light sources *Nat. Photon.* **1** 215–23
- [33] Kako S, Santori C, Hoshino K, Götzinger S, Yamamoto Y and Arakawa Y 2006 A gallium nitride single-photon source operating at 200 K *Nat. Mater.* **5** 887–92
- [34] Kress A, Hofbauer F, Reinelt N, Kaniber M, Krenner H J, Meyer R, Böhm G and Finley J J 2005 Manipulation of the spontaneous emission dynamics of quantum dots in two-dimensional photonic crystals *Phys. Rev. B* **71** 241304
- [35] Press D, Götzinger S, Reitzenstein S, Hofmann C, Löffler A, Kamp M, Forchel A and Yamamoto Y 2007 Photon antibunching from a single quantum-dot-microcavity system in the strong coupling regime *Phys. Rev. Lett.* **98** 117402
- [36] Förtsch M, Fürst J U, Wittmann C, Strekalov D, Aiello A, Chekhova M V, Silberhorn C, Leuchs G and Marquardt C 2013 A versatile source of single photons for quantum information processing *Nat. Commun.* **4** 1818
- [37] Ding X et al 2016 On-demand single photons with high extraction efficiency and near-unity indistinguishability from a resonantly driven quantum dot in a micropillar *Phys. Rev. Lett.* **116** 020401
- [38] Kuhlmann A V, Houel J, Ludwig A, Greuter L, Reuter D, Wieck A D, Poggio M and Warburton R J 2013 Charge noise and spin noise in a semiconductor quantum device *Nat. Phys.* **9** 570–5
- [39] Somaschi N et al 2015 Near optimal single photon sources in the solid state *Nat. Photon.* **10** 340–5
- [40] Patel R B, Bennett A J, Farrer I, Nicoll C A, Ritchie D A and Shields A J 2010 Two-photon interference of the emission from electrically tunable remote quantum dots *Nat. Photon.* **4** 632–5
- [41] Loredo J C et al 2016 Scalable performance in solid-state single-photon sources *Optica* **3** 433
- [42] Kimble H, Dagenais M and Mandel L 1977 Photon antibunching in resonance fluorescence *Phys. Rev. Lett.* **39** 691–5
- [43] Grangier P, Roger G and Aspect A 1986 Experimental evidence for a photon anticorrelation effect on a beam splitter: a new light on single-photon interferences *Europhys. Lett.* **1** 173–9
- [44] Filip R and Lachman L 2013 Hierarchy of feasible nonclassicality criteria for sources of photons *Phys. Rev. A* **88** 043827
- [45] Mari A and Eisert J 2012 Positive Wigner functions render classical simulation of quantum computation efficient *Phys. Rev. Lett.* **109** 230503
- [46] Lvovsky A, Hansen H, Aichele T, Benson O, Mlynek J and Schiller S 2001 Quantum state reconstruction of the single-photon Fock state *Phys. Rev. Lett.* **87** 050402
- [47] Straka I et al 2014 Robust quantum non-Gaussianity of single-photon states *Phys. Rev. Lett.* **113** 223603
- [48] Lasota M, Filip R and Usenko V C 2016 Sufficiency of quantum non-Gaussianity for discrete-variable quantum key distribution arXiv:1603.06620
- [49] Brown R H and Twiss R Q 1956 Correlation between photons in two coherent beams of light *Nature* **177** 27–9
- [50] Filip R and Mišta L 2011 Detecting quantum states with a positive Wigner function beyond mixtures of Gaussian states *Phys. Rev. Lett.* **106** 200401
- [51] Predojević A, Ježek M, Huber T, Jayakumar H, Kauten T, Solomon G S, Filip R and Weihs G 2014 Efficiency versus multi-photon contribution test for quantum dots *Opt. Express* **22** 4789–98
- [52] Slodička L, Hétet G, Röck N, Gerber S, Schindler P, Kumph M, Hennrich M and Blatt R 2012 Interferometric thermometry of a single sub-Doppler-cooled atom *Phys. Rev. A* **85** 043401
- [53] Eschner J, Raab C, Schmidt-Kaler F and Blatt R 2001 Light interference from single atoms and their mirror images *Nature* **413** 495–8
- [54] Almendros M, Huwer J, Piro N, Rohde F, Schuck C, Hennrich M, Dubin F and Eschner J 2009 Bandwidth-tunable single-photon source in an ion-trap quantum network *Phys. Rev. Lett.* **103** 213601
- [55] Takahashi H, Wilson A, Riley-Watson A, Oručević F, Seymour-Smith N, Keller M and Lange W 2013 An integrated fiber trap for single-ion photonics *New J. Phys.* **15** 053011
- [56] Schug M, Kurz C, Eich P, Huwer J, Müller P and Eschner J 2014 Quantum interference in the absorption and emission of single photons by a single ion *Phys. Rev. A* **90** 023829
- [57] Sinclair N et al 2014 Spectral multiplexing for scalable quantum photonics using an atomic frequency comb quantum memory and feed-forward control *Phys. Rev. Lett.* **113** 053603
- [58] Lachman L and Filip R 2013 Robustness of quantum nonclassicality and non-Gaussianity of single-photon states in attenuating channels *Phys. Rev. A* **88** 063841
- [59] Kurz C, Schug M, Eich P, Huwer J, Müller P and Eschner J 2014 Experimental protocol for high-fidelity heralded photon-to-atom quantum state transfer *Nat. Commun.* **5** 5527
- [60] Shu G, Kurz N, Dietrich M R and Blinov B B 2010 Efficient fluorescence collection from trapped ions with an integrated spherical mirror *Phys. Rev. A* **81** 042321
- [61] Streed E W, Norton B G, Jechow A, Weinhold T J and Kielpinski D 2011 Imaging of trapped ions with a microfabricated optic for quantum information processing *Phys. Rev. Lett.* **106** 010502
- [62] Fischer M, Bader M, Maiwald R, Golla A, Sondermann M and Leuchs G 2014 Efficient saturation of an ion in free space *Appl. Phys. B* **117** 797–801
- [63] Wong-Campos J D, Johnson K G, Neyenhuis B, Mizrahi J and Monroe C 2016 High resolution adaptive imaging of a single atom *Nat. Phot.* **10** 606–10
- [64] Streed E W, Jechow A, Norton B G and Kielpinski D 2012 Absorption imaging of a single atom *Nat. Commun.* **3** 933
- [65] Hillery M, O'Connell R F, Scully M O and Wigner E P 1984 Distribution functions in physics: fundamentals *Phys. Rep.* **106** 121–67
- [66] Yuen H P 1976 Two-photon coherent states of the radiation field *Phys. Rev. A* **13** 2226–43